九州大学学術情報リポジトリ
Kyushu University Institutional Repository

Determination of polycyclic aromatic hydrocarbons and their nitro-, amino-derivatives absorbed on particulate matter 2.5 by multiphoton ionization mass spectrometry using far-, deep-, and near-ultraviolet femtosecond lasers

Tang, Yuanyuan
Department of Applied Chemistry, Graduate School of Engineering, Kyushu University

Imasaka, Tomoko
Laboratory of Chemistry, Graduate School of Design, Kyushu University

Yamamoto, Shigekazu
Division of Air Science, Fukuoka Institute of Health and Environmental Sciences

Imasaka, Totaro
Department of Applied Chemistry, Graduate School of Engineering, Kyushu University

https://hdl.handle.net/2324/7170263

出版情報：Chemosphere. 152, pp.252-258, 2016-06. Elsevier
バージョン：
権利関係：

KYUSHU UNIVERSITY

Original Paper

Determination of polycyclic aromatic hydrocarbons and their nitro-, amino-derivatives absorbed on particulate matter 2.5 by multiphoton ionization mass spectrometry using far-, deep-, and near-ultraviolet femtosecond lasers

Yuanyuan Tang[a, *], Tomoko Imasaka[b], Shigekazu Yamamoto[c], Totaro Imasaka[a, d]

[a] *Department of Applied Chemistry, Graduate School of Engineering, Kyushu University, 744 Motooka, Nishi-ku, Fukuoka, 819-0395, Japan*

[b] *Laboratory of Chemistry, Graduate School of Design, Kyushu University, 4-9-1 Shiobaru, Minami-ku, Fukuoka 815-8540, Japan*

[c] *Division of Air Science, Fukuoka Institute of Health and Environmental Sciences, 39 Mukaizano Dazaifu, Fukuoka 818-0135, Japan*

[d] *Division of Optoelectronics and Photonics, Center for Future Chemistry, 744 Motooka, Nishi-ku, Fukuoka, 819-0395, Japan*

[*] Address reprint requests to Yuanyuan Tang

819-0395 744 Motooka, Nishi-ku, Fukuoka, Japan

TEL: +81-92-802-3295 FAX; +81-92-802-2888

E-mail address: tang.yuanyuan.398@s.kyushu-u.ac.jp (Y. Tang).

1. Introduction

A particulate matter with a diameter less than 2.5 μm, referred to as $PM_{2.5}$, is becoming a more serious problem in modern societies as the result of rapid urbanization and industrialization, especially in developing countries. Parent-polycyclic aromatic hydrocarbons (PPAHs) and their derivatives such as nitro-PAHs (NPAHs) and amino-PAHs (APAHs) are suspected to be components of $PM_{2.5}$. To date, the health risk posed by PAHs and their derivatives has already been assessed (Kim et al., 2013). It should be noted that NPAHs have indirect-acting mutagenicity and carcinogenicity for human beings, compared with direct-acting mutagenicity for PPAHs; up to 40% of the mutagen potency can be attributed to NPAHs especially to nitropyrene, dinitropyrene, and nitrohydroxypyrene (Albinet et al., 2006). Biologically-active APAHs influence human cells through different pathways compared to that of NPAHs (Øvrevik et al., 2010). The mutagenicities of aminofluoranthene (AFLU) and aminopyrene (APYR) have been proven to be the strongest among various types of two-, three-, and four-ring APAHs (Later et al., 1984). Therefore, exposure to the air containing $PM_{2.5}$ has become a major, world-wide concern for human health.

These PAH derivatives originate from different sources. Compounds such as PPAHs in $PM_{2.5}$ are generally produced by the incomplete combustion of the fossil fuel, municipal waste, and industrial organic matter. An alternative source for the generation of NPAHs would be a gas-phase reaction of the corresponding PPAHs and OH radicals in the presence of nitrogen oxide (NO_x) or a gas-particle heterogeneous reaction of ambient PPAHs that are adsorbed to the particle and $N_2O_5/NO_3/NO_2$ (Pitts et al., 1978). In comparison with NPAHs, APAHs are used as intermediates in industrial processes, suggesting that APAHs are mainly artificially synthesized. For example, APAHs have

been employed in the manufacturing of synthetic polymers, dyes, rubbers, pharmaceuticals, and pesticides, as well as for use as hair dyes, and are also produced from cigarette smoke and automobile exhaust (Vlastimil et al., 2011). They can also be generated from NPAHs as reduction products in the presence of the catalyst used for purifying exhaust gas produced from diesel engines.

The mutagenic effects of NPAHs are strongly enhanced in the presence of PPAHs. Although the concentrations of NAPHs in $PM_{2.5}$ are very low (~ pg/m^3) (Hayakawa et al., 2014), their toxicities range from several times to one hundred thousand times higher than those of the corresponding PPAHs (Wang et al., 2011). Since numerous interfering organic species are present in $PM_{2.5}$, a sensitive and selective analytical method is needed for the determination of NPAHs. Several analytical techniques, based on gas chromatography (GC) coupled with mass spectrometry (MS) and high performance liquid chromatography (HPLC) coupled with chemiluminescence (CL) and fluorescence (FL) detections, have been used for the analysis of PPAHs, NPAHs, and APAHs in complex matrices (Hayakawa et al., 2000). However, there are several limitations to these established methods: the dominant fragmentation in electron-ionization MS and the use of an additional column for reducing NPAHs to the corresponding APAHs in CL and FL (Li et al., 1994; Ohno et al., 2009). Laser desorption ionization/mass spectrometry (LDI/MS) has been extensively studied for the analysis of NPAHs (Dotter et al., 1996; Tasker et al., 2003). However, nitro group in NPAHs tends to destruct the π ring system. The electron-deficient nature influences the ionization and fragmentation processes. It has been reported that NPAHs showed strong fragments when a nanosecond laser pulse was used (Dotter et al., 1996). Such fragmentation can be suppressed using a femtosecond laser pulse (Matsumoto et al.,

1997; Tasker et al., 2003), which can be explained by the ladder-switching mechanism (Ledingham et al., 1997). These results suggest that a femtosecond laser is desirable for observing a molecular ion and for trace analysis of NPAHs. In our previous study, GC was combined with time-of-flight MS (TOFMS) using a femtosecond laser as the ionization source. Femtogram detection limits were achieved and the instrument was applied for the trace analysis of PAHs and NPAHs (Tang et al., 2015). The present technique has several advantages; the two-dimensional display of GC-MS can be used for comprehensive analysis, and the analytes can be more selectively and softly ionized through the multiphoton ionization (MPI) process (Boesl et al., 1994). For this reason, it is desirable to investigate the ionization efficiency of NPAHs and APAHs in GC-MPI/TOFMS using a femtosecond laser.

In this study, GC-MPI/TOFMS was applied to the determination of PPAHs, NPAHs, and APAHs. In MPI, the laser wavelength plays an important role in enhancing the sensitivity and in suppressing fragmentation and background noise due to their different absorption characters. Therefore, lasers emitting at three different wavelengths were used to study the ionization mechanisms, e.g., resonance-enhanced two-photon ionization (RE-2PI), resonance-enhanced three-photon ionization (RE-3PI), and non-resonant two-photon ionization (NRE-2PI). Although numerous spectral data are available for PAHs and their derivatives, they are not sufficient to permit a valid comparison to be made. For example, data concerning ionization energies and ionization efficiencies at different wavelengths are not available. This is particularly true in the case of MPI using a femtosecond laser. It has been reported that the signal intensity and the detection limit can be improved substantially using the fourth harmonic emission (200 nm) rather than the third harmonic emission (267 nm)

(Hashiguchi et al., 2013). Because of this, a far-ultraviolet laser (200 nm) was used to investigate the ionization mechanism for PPAHs, NPAHs, and APAHs in order to optimize the ionization efficiency. To our knowledge, this is the first report for the determination of three different types of PAHs, i.e., PPAHs (plane), NPAHs (oxidative), and APAHs (reductive) in $PM_{2.5}$, using a femtosecond laser as the ionization source in MS.

2. Experimental

2.1. Analytical Instrument

Details of the GC-MPI/TOFMS used in this study have been reported elsewhere (Imasaka, 2013). A block diagram of the setup is shown in Fig. S1. Briefly, a GC system (6890N, Agilent technologies) equipped with an auto sampler (7683B, Agilent Technologies) was combined with a TOFMS developed in our laboratory, which is now commercially available (HGK-1, Hikari-GK, Fukuoka, Japan). A DB-5MS column (30 m long, 0.25 mm inner diameter, 0.25 μm film thickness) was used for the separation of the analytes. The temperature of the GC oven for the analysis of the standard sample mixture containing three PPAHs and three NPAHs was programed from 50 ºC, a 1-min hold, to 220 ºC at a rate of 10 ºC/min and finally increased to 310 ºC at a rate of 5 ºC/min, then a 2 min hold, according to a protocol reported in the literature (Tang et al., 2015). The total elution time was 38 min. In order to reduce the time required for the measurement, a different temperature program was utilized for the separation of the APAHs, the total time for the GC separation being 14.5 min. The temperature program

was as follows: the initial temperature was 60 ºC, 1 min hold, then the temperature was increased at a rate of 40 ºC/min to 200 ºC, then at 2 ºC/min to 280 ºC, followed by a 6 min hold (Kinouchi et al., 1990). The temperature of the sample inlet port and the transfer line connecting the GC and the MS were set at 300 and 250 ºC, respectively. The flow rate of helium used as a carrier gas was maintained at 1 mL/min. A 1-μL aliquot of the sample solution was injected into a GC using the splitless-injection method. The analytes separated by GC were introduced into the MS as a molecular beam for MPI. The produced ions were accelerated into a flight tube by the potentials applied to the electrodes to reach a microchannel plate detector (F4655-11, Hamamatsu Photonics). The signal was recorded by a computer-interfaced digitizer (Acqiris AP240, Agilent Technologies), and the data were processed using the LabVIEW software program.

An optical parametric amplifier (OPA, OPerA-Solo, Coherent Co.) was pumped by the fundamental beam of a Ti:sapphire laser (800 nm, 35 fs, 1 kHz, 4 mJ, Elite, Coherent Co.) to generate a near-ultraviolet femtosecond pulse (345 nm). As shown in Fig. 1, the fundamental beam emitting at 800 nm was introduced into a harmonic generator for the second harmonic generation (SHG, 400 nm), the third harmonic generation (THG, 267 nm), and the fourth harmonic generation (FHG, 200 nm). The energy for the laser pulse was adjusted to 12 ± 1 μJ for a comparison of the ionization efficiency. The laser beam was focused with a concave mirror into a molecular beam for MPI. The ultraviolet-visible (UV-vis) absorption spectra were recorded for PPAHs, NPAHs, and APAHs using a spectrophotometer (Jasco model V-650).

2.2. Standard samples

Standard samples of PPAHs, i.e., anthracene (ANT), fluoranthene (FLU), pyrene (PYR), were supplied by Wako Pure Chemical Industries. Ltd. A standard sample mixture containing 9-nitro-ANT (9-NANT), 3-nitro-FLU (3-NFLU), and 1-nitro-PYR (1-NPYR) dissolved in toluene (100 ng/μL for each compound) was purchased from AccuStandard Inc. Compounds of 3-amino-FLU (3-AFLU) and 1-amino-PYR (1-APYR) were purchased from Sigma-Aldrichand and 9-amino-ANT (9-AANT) from Angene International Limited. It should be noted that freshly prepared 9-AANT was utilized in this study due to the instability of this compound. The molecular structures of these compounds are shown in Fig. S2. Dichloromethane (analytical grade) and acetonitrile (LC-MS grade) obtained from Wako Pure Chemical Industries. Ltd. were used to extract the analytes and to dissolve the standard samples of PPAHs and NPAHs, respectively. Methanol (analytical grade) obtained from Wako Pure Chemical Industries. Ltd. was used as the solvent for the APAHs due to the insolubility of 9-AANT in acetonitrile. Standard sample solutions of PPAHs and APAHs were prepared at a concentration of 10 ng/μL for each. The standard sample mixture containing three PPAHs (200 pg/μL) and three NPAHs (500 pg/μL) was obtained by diluting the standard sample solutions using acetonitrile as a solvent. A sample mixture containing three APAHs was prepared at a concentration of 200 pg/μL for each using methanol as the solvent. For the measurement of the absorption spectrum, the PPAHs, NPAHs, and APAHs were all prepared at a concentration of 10 ng/μL for each. The NPAHs samples were further diluted to 100 pg/μL to avoid saturation of the signal at around 200 nm.

2.3. Pretreatment of $PM_{2.5}$

The procedures for sampling and pretreatment have been described in a previous report (Tang et al., 2015). Briefly, the sampling site was located on the roof of a building, which was about 16.4 m above the ground, at the Fukuoka Institute of Health and Environmental Sciences. A filter (effective area, 18 × 23 cm^2, Tissuquartz 2500QAT-UP, Pallflex Air Monitoring Filters, Pall Corporation) was used to collect the $PM_{2.5}$ from 9:00 AM on 1. July. 2014 to 8:50 AM on 2. July. 2014 at a flow rate of 740 L/min. The total sampling time was 1430 min. The amount of $PM_{2.5}$ collected during this period was 58.7 mg and the concentration of the $PM_{2.5}$ was 55.5 $\mu g/m^3$.

A part of the filter (6 ×6 cm^2) was cut into small pieces, and the analytes were ultrasonically extracted three times (15 minutes for each extraction) with 10 mL of dichloromethane. Methanol (1 mL) was added as a solvent after removing dichloromethane by a stream of nitrogen gas. A syringe with a membrane filter (GL-13N, pore size 0.2 μm, GL-Science. Inc) was then used to remove small particles, which was then concentrated to 50 μL using a stream of nitrogen gas. All of the prepared samples were stored in a refrigerator until analysis.

2.4. Quantum chemical calculations

To investigate the ionization mechanism of PPAHs, NPAHs, and APAHs, quantum chemical calculations were performed for PPAHs and APAHs, as reported previously for NPAHs using a Gaussian09 program series package. Geometries were calculated using the B3LYP method based on density functional theory (DFT) with a cc-pVDZ basis set (Dunning et al., 1989). The harmonic frequencies were calculated to ensure an

optimum geometry providing a global energy minimum. A vertical ionization energy (*IE*) was calculated from the difference between the energies of the ground and ionic states, which were obtained at the level of B3LYP/cc-pVTZ. The lowest forty singlet transition energies (*EE*) and the oscillator strengths were calculated using time-dependent DFT (TD-DFT) (Bauernschmitt et al., 1996), and the predicted absorption spectra were also generated using the Gauss View 5 software program by assuming a Gaussian-profile peak with a half width at half maximum of 0.333 eV.

3. Results and discussion

3.1. Absorption spectrum

Ionization efficiency is dependent on the laser wavelength used in MPI. Ionization efficiency can be drastically increased when the laser wavelength is adjusted to that for one of the absorption bands. This favorable effect provides additional selectivity in MPI/MS. A UV-vis absorption spectrum was measured for PPAHs, NPAHs, and APAHs under the same conditions for comparison. The results, which are shown in Fig. S3, are in good agreement with the reported data (Joseph et al., Varian® Application Note No. 8; Catalfo et al., 2008); the absorption spectra measured in the condensed phase were shifted by 6-18 nm toward shorter wavelengths compared to that for the gaseous phase (Li et al., 2010). As recognized from the spectra shown in Fig. S3 and the calculated spectra shown in Fig. S4, ANT and its derivatives (NANT and AANT) have large molar absorptivities at around 250 nm but small values at around 350 and 200 nm. On the other hand, the other compounds such as FLU and PYR, NFLU and NPYR, and

AFLU and APYR have larger molar absorptivities at around 350 and 200 nm. These results suggest that these compounds would be efficiently ionized through a process of resonance-enhanced multiphoton ionization (REMPI) at 200 nm using the fourth harmonic emission (200 nm) of a Ti:sapphire laser. Such a laser, emitting in the far-ultraviolet, has been reported to be useful for enhancing sensitivity in pesticide analyses (Hashiguchi et al., 2013). On the other hand, a near-ultraviolet femtosecond laser (345 nm) has been successfully used to reduce the background signals from interfering species contained in an actual sample (Tang et al., 2015).

3.2. Ionization mechanism

The calculated ionization energies of the PPAHs, NPAHs, and APAHs are shown in Table 1. Among them, APAHs have relatively lower ionization energies compared with those for PPAHs and NPAHs. It is evident that the nitro group withdraws π electrons and increases the ionization energy for NPAHs, while an amino group donates its lone-pair of electrons, resulting in a reduction in the ionization energies for APAHs. The same phenomena have been reported for nitro- and amino-substituted benzenes (Crable et al., 1962), which is explained by a difference in energy for the interaction between the induced dipole and the charge center and between the permanent dipole and the charge center for an electron-withdrawing group, such as $-NO_2$, and the electron-donating group of $-NH_2$ (Crable et al., 1962).

The mechanism of ionization was investigated using data regarding ionization energy and the first excitation energy. The photon energies for lasers emitting at 200,

267, and 345 nm are calculated to be 6.19, 4.64, and 3.59 eV, respectively. The PAHs can then be ionized through a process of RE-2PI at the wavelengths of 200 and 267 nm. When the laser wavelength is adjusted to 345 nm, a different type of ionization scheme appears, due to the lower photon energy. For example, NPAHs and FLU would be ionized through a process of RE-3PI due to their higher ionization energies than the other compounds. It is noteworthy that PYR would be ionized by NRE-2PI due to a higher excitation energy for the first electronic-excited state, suggesting that the sensitivity is low for PYR in the case of an MS measured at 345 nm. Although RE-2PI is operative for APAHs due to their lower ionization energies at these wavelengths, the excess energies would decrease with an increase in laser wavelength. This suggests that fragmentation can be suppressed by using a laser emitting at longer wavelengths.

3.3. Two-dimensional display

The analyte molecule can be ionized, when the sum of the absorbed photon energy exceeds the ionization energy. In addition, the efficiency of MPI can be improved when a target molecule can be ionized via an intermediate excited state. Then, the ionization efficiency would be enhanced at the optional laser wavelength. For this reason, two-dimensional data of GC-MPI/TOFMS were measured for three groups of PAHs at 200, 267, and 345 nm. The two-dimensional display obtained at 200 nm is shown in Fig. 1. Several fragment ions appear for the NPAHs, which is in contrast to the other PPAHs and APAHs. In our previous study, NPAHs, especially NFLU and NPYR, were found to be susceptible to decomposition at high temperature (300 ºC) (Tang et al., 2015). The thermal decomposed products can be assigned to their corresponding APAHs, which is

in good agreement with previously reported data (Sweetman et al., 1982). It should be noted that the signals of APAHs did not appear at the retention times of NPAHs but appeared at those of APAHs. In addition, the signals of the decomposition products decreased with decreasing temperature of the sample injection port. Then, the decomposition would occur in the sample injection port of the GC, which is in contrast to a previous report indicating that the analyte molecules decomposed in the electron-ionization source of the MS (Sweetman et al., 1982). Although the decomposition products were significantly suppressed or even completely eliminated by decreasing the temperature, the signal intensities of the NPAHs decreased drastically, probably due to insufficient vaporization in the sample injection port and to the broadening of the peaks in the chromatogram. For this reason, the high temperature of the inlet port was retained in this study. It would be possible to avoid such decompositions of NPAHs using a solvent that contains no hydrogen atoms, since the acetonitrile used as a solvent is only a source of hydrogen atoms to produce APAHs.

The detection limits (DLs) of PPAHs, NPAHs, and APAHs measured in this study are summarized in Table S1. They are in the range of 0.06～1.17, 0.20～1.19, and 0.07～0.48 pg for these compounds, respectively. The DLs of NPAHs were much lower than the data (e.g., 30 pg for 1-NPYR) obtained by GC coupled with negative ion chemical ionization MS (GC/NICIMS) using a derivatization technique (Xu et al., 2001). The DL of 1-NPYR was improved to 0.17 pg in GC/MS using a programmed temperature vaporization (PTV) injector (Crimmins and Baker, 2006), the value of which is comparable to the value of 0.20 pg obtained in this study. On the other hand, the DL was reported to be 18 pg for 3-AFLU (Farant et al., 2002), which is in contrast

to the value of 0.074 pg acheived in this study. These results suggest that the sensitivity of the present instrument is similar or superior to those of GC/MS currently used in environmental analysis.

3.4. Ionization efficiency

Mass chromatograms obtained by extracting data from the two-dimensional display measured at three different wavelengths are shown in Fig. S5. The intensities of the signal peaks calculated from their mass chromatograms are compared in Fig. 2. The standard deviation was calculated from the three independent data, suggesting sufficient reproducibility in GC/MS for quantitative analysis. The reported lifetimes of the singlet-excited states of the PPAHs, NPAHs, and APAHs in the condensed phase as well as in the gas phase are summarized in Table 1. Thus, the pulse width of the femtosecond laser is apparently shorter than the excited-state lifetimes of the PPAHs and APAHs and nearly equal to, or slightly shorter than the lifetimes of the NPAHs. This can be attributed to efficient intersystem crossing for the NPAHs, which would result in a decrease in ionization efficiency. As shown in Fig. 2, the order of the ionization efficiencies were found to be PPAHs>APAHs>NPAHs at these three wavelengths, although there are some exceptions; AFLU and APYR were ionized more efficiently than FLU and PYR at 345 nm, respectively. This result can be explained by the ionization mechanism. Although AFLU and APYR are ionized through an efficient RE-2PI process, FLU and PYR are ionized through less efficient RE-3PI and NRE-2PI processes, respectively. Thus, ionization efficiency is dependent on the ionization mechanism. It should be noted that all of these compounds were ionized most efficiently

at 200 nm, which is in good agreement with the predicted data from the absorption spectra. It is interesting to note that the difference in ionization efficiency for the data measured at 267 and 345 nm was within a factor of 2 for these compounds, except for FLU and PYR, even though NPAHs are ionized through RE-2PI at 267 nm and are ionized through RE-3PI at 345 nm. For FLU and PYR, the higher ionization efficiencies measured at 267 nm can be explained by the RE-2PI process, which is more efficient than RE-3PI and NRE-2PI at 345 nm. Similar ionization efficiencies measured for NPAHs at 267 nm (RE-2PI) and 345 nm (RE-3PI) can be explained by the shorter (267 nm) and longer (345 nm) lifetimes relative to the pulse width of the femtosecond laser, although no lifetime data are available in the literature. It is noteworthy that NANT shows relatively low ionization efficiencies, probably owing to a symmetric chemical structure, which would result in lower molar absorptivities at these wavelengths.

3.5. Measurement of $PM_{2.5}$

A sample extracted from $PM_{2.5}$ was measured to evaluate the advantage of GC-MPI/TOFMS in practical trace analysis. The observed two-dimensional displays are shown in Fig. 3. Although a higher ionization efficiency was obtained at 200 nm, numerous contaminants probably arising from unknown PPAHs were present, making the identification of NPAHs difficult. It appears that the background signal can be suppressed at longer wavelengths. Thus, a laser emitting at 345 nm would be more useful for the sensitive and selective determination of toxic NPAHs in the environmental samples. On the other hand, a laser emitting at 200 nm would be more useful for a sample that had been cleaned up carefully because of its superior sensitivity.

Their expanded views and the mass chromatograms are shown in Fig. 4. All the target compounds except 9-AANT were detected and identified at 345 nm probably due to the instability of this compound and then its low concentration in the atmosphere. It should be noted that multiple peaks are observed in Fig. 4 (c). A pair of them can be assigned to 3-AFLU and 1-APYR and the other pair to the fragment peaks of 3-NFLU and 1-NPYR (see the caption of Fig. 4). The concentrations of 9-NANT, 3-NFLU, and 1-NPYR were determined to be 12, 8, and 9 pg/m^3, respectively, from the data shown in Fig. 4. The concentrations of ANT, FLU, and PYR were 6, 25, and 22 pg/m^3, respectively. Some portions of the signals assigned to 3-AFLU and 1-APYR could have been produced by the thermal decomposition of NPAHs in the sample injection port of the GC. Their contributions were limited to 8 and 14 % of 3-NFLU and 1-NPYR for 3-AFLU and 1-APYR, respectively, which were calculated from data obtained using standard samples. The ratios of the signal intensities for 3-AFLU/3-NFLU and 1-APYR/1-NPYR observed in Fig. 4 were 1.3 and 1.4, respectively, and the contribution of the decomposition products appear to be negligibly small in this study. Then, the concentrations of 3-AFLU and 1-APYR were calculated to be 5 and 4 pg/m^3, respectively, which were obtained by neglecting the contribution of the peaks arising from the fragments of 3-NFLU and 1-NPYR (see Fig. 4 (c)). It should be noted that the APAHs were directly determined in this study by means of GC/MPI/TOFMS without using a chemical reaction for derivatization (Bakthavachalam et al., 1990).

4. **Conclusion**

The ionization mechanism was investigated by measuring PPAHs, NPAHs, and APAHs at three different wavelengths of 200, 267, and 345 nm and by using data from their absorption spectra and ionization energies. The largest ionization efficiency was achieved at 200 nm due to the largest molar absorptivity for a transition to a singlet-electronic-excited state through the most efficient process of RE-2PI. On the other hand, a laser emitting in the near-ultraviolet region, i.e., 345 nm, was found to be useful for suppressing the undesirable background signals arising from interfering species, thus allowing the trace analysis of the target molecules in the sample extracted from $PM_{2.5}$. As demonstrated herein, GC/MPI/TOFMS using a UV femtosecond laser as ionization source has a potential for use in the practical trace analysis of a family of PAHs in the environment.

Acknowledgments

This research was supported by a Grant-in-Aid for Scientific Research from the Japan Society for the Promotion of Science (JSPS KAKENHI Grant Number 26220806, 15K13726, and 15K01227). We wish to thank Vu Duong, Atsushi Mori, and Yuichiro Kida for their contributions in the generation and operation of the femtosecond laser emitting at 200 nm. We also wish to thank Adan Li for discussions of the results. The quantum chemical calculations were mainly carried out using the computer facilities at the Research Institute for Information Technology, Kyushu University.

References

Albinet, A., Leoz-Garziandia, E., Budzinski, H., Villenave, E., 2006. Simultaneous analysis of oxygenated and nitrated polycyclic aromatic hydrocarbons on standard reference material 1649a (urban dust) and on natural ambient air samples by gas chromatography-mass spectrometry with negative ion chemical ionization. J. Chromatogr. A 1121, 106-113.

Boesl, U., Zimmermann, R., Weickhardt, C., Lenoir, D., Schramm, K.W., Kettrup, A., Schlag, E.W., 1994. Resonance-enhanced multi-photon ionization: a species-selective ion source for analytical time-of-flight mass spectroscopy. Chemosphere 29, 1429-1440.

Bauernschmitt, R., Ahlrichs, R., 1996. Treatment of electronic excitations within the adiabatic approximation of time dependent density functional theory. Chem. Phys. Lett. 256, 454-464.

Bakthavachalam, J., Annan, R.S., Beland, F.A., Vouros, P., Giese, R.W., 1990. Selection of electrophoric derivatives of 1-aminopyrene and 2-aminofluorene for determination by gas chromatography with electron-capture negative-ion mass spectrometry. J. Chromatogr. 500, 373-386.

Chakraborti, H., Brmhaiah, K., John, N.S., Pal, S.K., 2013. Excited state electron transfer from aminopyrene to graphene: a combined experimental and theoretical study. Phys. Chem. Chem. Phys. 15, 19932-19938.

Catalfo, A., Serrentino, M.E., Librando, V., Perrini, G., Guidi, G.D., 2008. Spectroscopic properties of some derivatives of polycyclic aromatic hydrocarbons. Appl. Spectrosc. 62, 1233-1237.

Crable, G.F., Kearns, G.L., 1962. Effect of substituent groups on ionization potentials of benzenes. J. Phys. Chem. 66, 436-439.

Crimmins, B.S., Baker, J.E., 2006. Improved GC/MS methods for measuring hourly PAH and nitro-PAH concentrations in urban particulate matter. Atmospheric Environ. 40, 6764-6779.

Dunning Jr., T.H., 1989. Gaussian-basis sets for use in correlated molecular calculations. Ⅰ. The atoms boron through neon and hydrogen. J. Chem. Phys. 90, 1007-1023.

Dotter, R.N., Smith, C.H., Young, M.K., Kelly, P.B., Daniel Jones, A., McCauley, E.M., Chang, D.P.Y., 1996. Laser desorption/ionization time-of-flight mass Spectrometry of nitrated polycyclic aromatic hydrocarbons. Anal. Chem. 68, 2319-2324.

Farant, J.P., Ogilvie, D., 2002. Investigation of the presence of amino and nitro polycyclic aromatic hydrocarbons in a söderberg primary aluminum smelter. Am. Ind. Hyg. Asosoc. J. 63, 721-725.

Hashiguchi, Y., Zaitsu, S., Imasaka, T., 2013. Ionization of pesticides using a far-ultraviolet femtosecond laser in gas chromatography/time-of-flight mass spectrometry. Anal. Bioanal. Chem. 405, 7053-7059.

Hayakawa, K., 2000. Chromatographic methods for carcinogenic/mutagenic nitropolycyclic aromatic hydrocarbons. Biomed. Chromatogr. 14, 397-405.

Hayakawa, K., Tang, N., Kameda, T., Toriba, A., 2014. Atmosphere behaviors of polycyclic aromatic hydrocarbons in East Asia. Gene. Environ. 36, 152-159.

Joseph, M., Identification of polynuclear aromatic hydrocarbons in a complex matrix with diode array detection. In Varian Application Note Number 8. Available online: <https://www.agilent.com/cs/library/applications/lc08.pdf>

Kim, K.H., Jahan, S.A., Kabir, E., Brown, R.J.C., 2013. A review of airborne polycyclic aromatic hydrocarbons (PAHs) and their human health effects. Environ. Int. 60, 71-80.

Kinouchi, T., Miranda, A.T.L., Rushing, L.G., Beland, F.A., Korfmacher, W.A., 1990. Detection of 2-aminofluorene at femtogram levels via high-resolution gas-chromatography combined with negative-ion atmospheric-pressure ionization mass-spectrometry. J. High Resolut. Chromatogr. 13, 281-284.

Later, D.W., Pelroy, R.A., Stewart, D.L., McFall, T., Booth, G.M., Lee, M.L., Tedjamulia, M., Castle, R.N., 1984. Microbial mutagenicity of isomeric two-, three-, and four-ring amino polycyclic aromatic hydrocarbons. Environ. Mutagen. 6, 497-515.

Li, H., Westerholm, R., 1994. Determination of mono- and di-nitro polycyclic aromatic hydrocarbons by on-line reduction and high-performance liquid chromatography with chemiluminescence detection. J. Chromatogr. A 664, 177-182.

Ledingham, K.W.D., Singhal, R.P., 1997. High intensity laser mass spectrometry-a review, Int. J. Mass Spectrom. Ion Process 163, 149-168.

Li, A., Uchimura, T., Tsukatani, H., Imasaka, T., 2010. Trace analysis of polycyclic aromatic hydrocarbons using gas chromatography-mass spectrometry based on nanosecond multiphoton ionization. Anal. Sci. 26, 841-846.

Matsumoto, J., Lin, C.H., Imasaka, T., 1997. Supersonic jet multiphoton ionization mass spectrometry using nanosecond and femtosecond pulse lasers. Anal. Chim. Acta 343, 129-133.

Morales-Cueto, R., Esquivelzeta-Rabell, M., Saucedo-Zugazagoitia, J., Peon, J., 2007. Singlet excited-state dynamics of nitropolycyclic aromatic hydrocarbons: direct

measurements by femtosecond fluorescence up-conversion. J. Phys. Chem. A 111, 552-557.

Murov, S.L., Carmichael, I., Hug, G.L., 1993. “Handbook of photochemistry”, 2nd ed., New York.

Øvrevik, J., Arlt, V.M., Øya, E., Nagy, E., Mollerup, S., Phillips, D.H., Låg, M., Holme, J.A., 2010. Differential effects of nitro-PAHs and amino-PAHs on cytokine and chemokine responses in human bronchial epithelial BEAS-2B cells. Toxicol. Appl. Pharmacol. 242, 270-280.

Ohno, T., Toriba, A., Kameda, T., Tang, N., Hayakawa, K., 2009. Determination of 1-nitropyrene in low volume ambient air samples by high-performance liquid chromatography with fluorescence detection. J. Chromatogr. A 1216, 4625-4628.

Pitts Jr., J.N., Van Cauwenberghe, K.A., Grosjean, D., Schmid, J.P., Fitz, D.R., Belser Jr., W.L., Knudson, G.P., Hynds, P.M., 1978. Atmospheric reactions of polycyclic aromatic hydrocarbons: facile formation of mutagenic nitro derivatives. Science 202, 515-519.

Sweetman, J.A., Karasek, F.W., Schuetzle, D., 1982. Decomposition of nitropyrene during gas-chromatographic mass-spectrometric analysis of air particulate and fly-ash samples, J. Chromatogr. A 247, 245-254.

Tasker, A.D., Robson, L., Ledingham, K.W.D., McCanny, T., McKenna, P., Kosmidis, C., Jaroszynski, D.A., 2003. Femtosecond ionization and dissociation of laser desorbed nitro-PAHs. Int. J. Mass Spectrom. 225, 53-70.

Tang, Y., Imasaka, T., Yamamoto, S., Imasaka, T., 2015. Multiphoton ionization mass spectrometry of nitrated polycyclic aromatic hydrocarbons. Talanta 140, 109-114.

Tang, N., Hattori, T., Taga, R., Igarashi, K., Yang, X., Tamura, K., Kakimoto, H., Mishukov, V.F., Toriba, A., Kizu, R., Hayakawa, K., 2005. Polycyclic aromatic hydrocarbons and nitropolycyclic aromatic hydrocarbons in urban air particulates and their relationship to emission sources in the Pan–Japan Sea countries. Atmos. Environ. 39, 5817-5826.

Vlastimil, V., Jiri, B., 2011. Electroanalysis of nitro and amino derivatives of polycyclic aromatic hydrocarbons. Curr. Org. Chem. 15, 3059-3076.

Wang, W., Jariyasopit, N., Schrlau, J., Jia, Y., Tao, S., Yu, T.W., Dashwood, R.H., Zhang, W., Wang, X., Simonich, S.L.M., 2011. Concentration and photochemistry of PAHs, NPAHs, and OPAHs and toxicity of PM2.5 during the beijing olympic games. Environ. Sci. Technol. 45, 6887-6895.

Xu, J., Lee, F.C., 2001. Analysis of nitrated polycyclic aromatic hydrocarbons. Chemosphere 42, 245-250.

Table 1 Characteristics of PPAHs, NPAHs, and APAHs.

Compounds	Abbreviation	Mw	Formula	*IE* (eV)	τ_c (fs)	τ_g (fs)
Anthracene	ANT	178	$C_{14}H_{10}$	7.11	[a] 6×10^6	[a] 6×10^6
Fluoranthene	FLU	202	$C_{16}H_{10}$	7.60	[a] 5.3×10^7	[a] 3.8×10^7
Pyrene	PYR	202	$C_{16}H_{10}$	7.16	[a] 6.5×10^8	[a] 1.4×10^9
9-nitroanthracene	9-NANT	223	$C_{14}H_9NO_2$	7.59	[b] 60	--
3-nitrofluoranthene	3-NFLU	247	$C_{16}H_9NO_2$	8.06	[b] 50	--
1-nitropyrene	1-NPYR	247	$C_{16}H_9NO_2$	7.67	[b] 540	--
9-aminoanthracene	9-AANT	193	$C_{14}H_9NH_2$	6.60	[c] 10×10^6	--
3-aminofluoranthene	3-AFLU	217	$C_{16}H_9NH_2$	6.75	--	--
1-aminopyrene	1-APYR	217	$C_{16}H_9NH_2$	6.64	[d] 5.7×10^6	--

IE, ionization energy; τ_c and τ_g are the lifetimes measured in the condensed and gaseous phases, respectively; "--" no references are available.

[a] Ref. (Li et al., 2010).

[b] Ref. (Morales-Cueto et al., 2007).

[c] Ref. (Chakraborti et al., 2013).

[d] Ref. (Murov et al., 1993).

Figure Captions

Fig. 1. Two-dimensional displays of the standard sample mixture; (a) PPAHs + NPAHs (b) APAHs. Wavelength, 200 nm; pulse energy, 12 ± 1 μJ. The signals of APAHs observed in (a) are due to the thermal decomposition of NPAHs in the sample injection port of the GC.

Fig. 2. The averaged peak heights of the molecular ions calculated from the mass chromatograms (Fig. S3). Data measured for PPAHs, NPAHs, and APAHs measured at 200, 267, and 345 nm. The error bars show the standard deviation of the signal peaks for molecular ions.

Fig. 3. Two-dimensional displays of the sample extracted from $PM_{2.5}$. Laser wavelength; (a) 200 (b) 267 (c) 345 nm. Pulse energy, 12 ± 1 μJ for (a) (b) (c).

Fig. 4. Expanded views of the data shown in Fig. 3 (c) and accompanying mass chromatograms of NPAHs and APAHs. Laser wavelength, 345 nm. The signals specified by F_1 and F_2 in (c) can be assigned to the fragment ions arising from 3-NFLU and 1-NPYR, respectively (see Fig. 1).

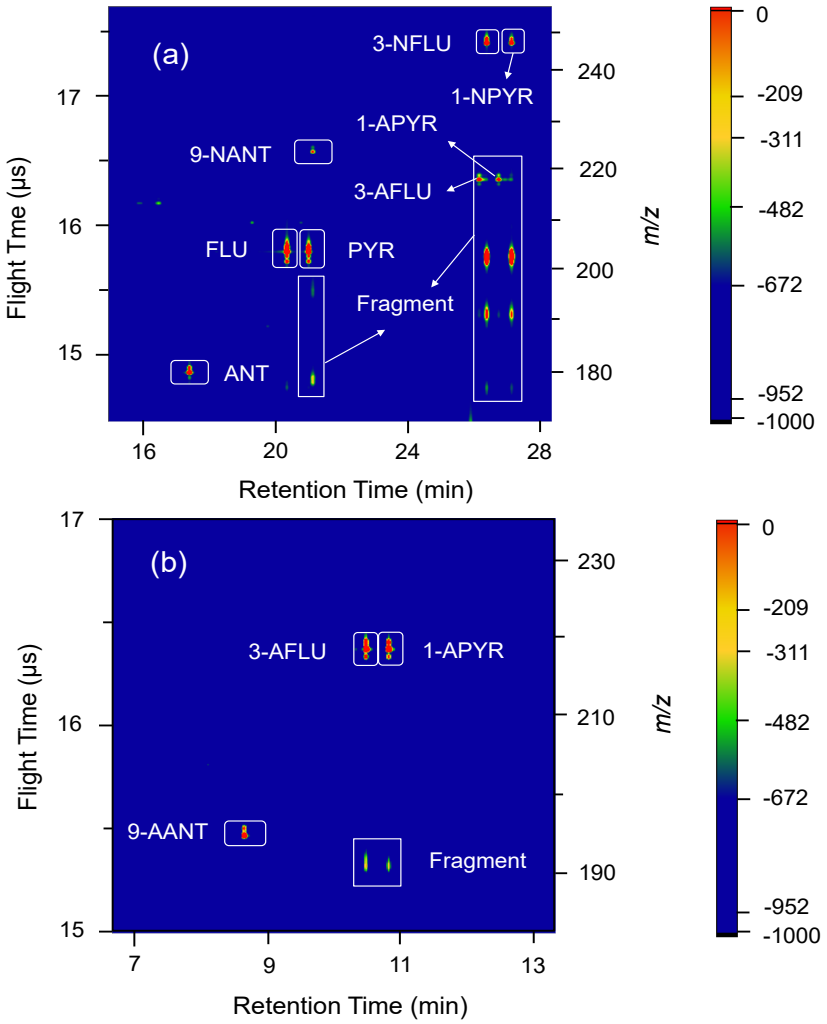

Fig. 1 Y. Tang et al.

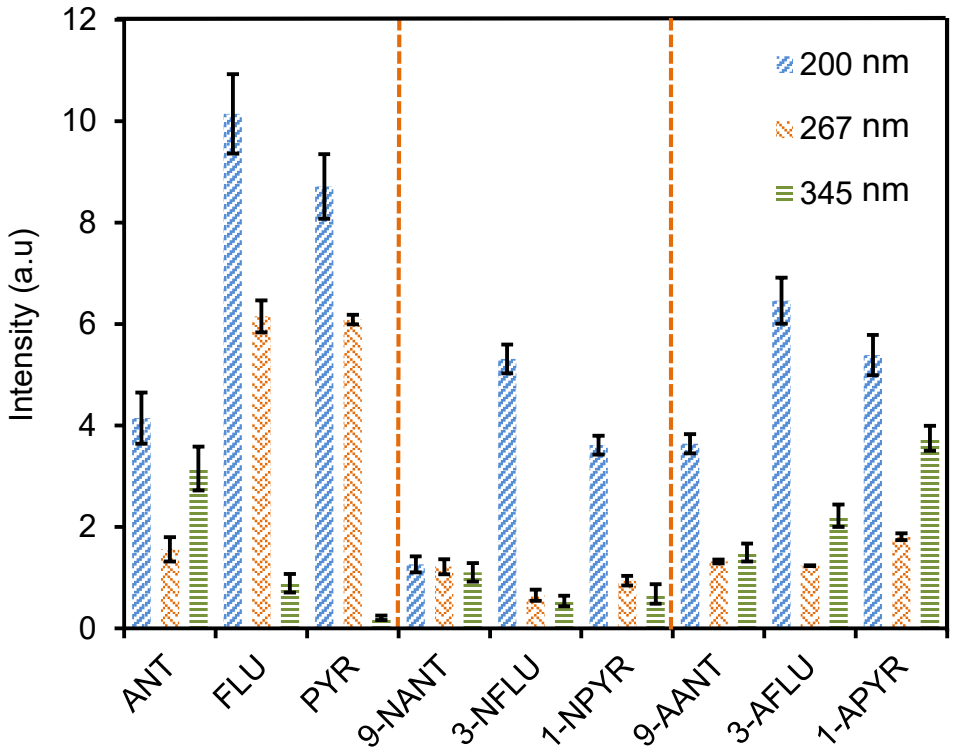

Fig. 2 Y. Tang et al.

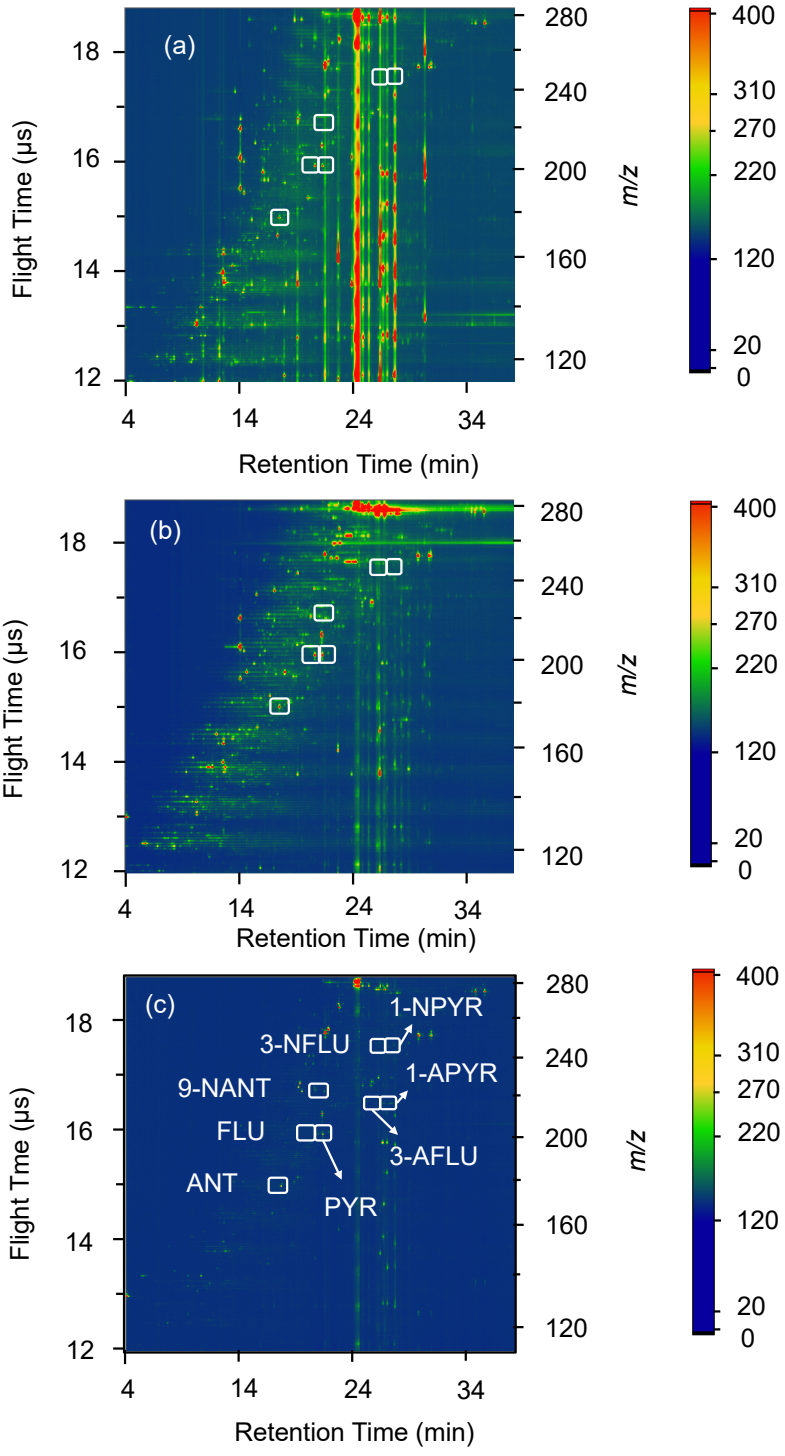

Fig. 3 Y. Tang et al.

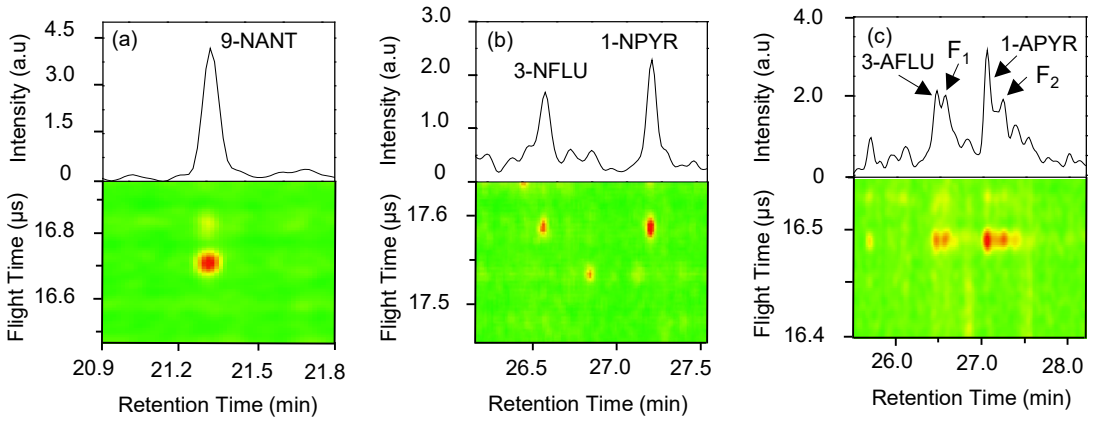

Fig. 4 Y. Tang et al.